Available online at www.sciencedirect.com

ScienceDirect

Ceramics International 40 (2014) 1117–1123

CERAMICS INTERNATIONAL

www.elsevier.com/locate/ceramint

High temperature X-ray studies of mayenite synthesized using the citrate sol–gel method

Sabina N. Ude[a], Claudia J. Rawn[a,b,*], Roberta A. Peascoe[b], Melanie J. Kirkham[c], Gregory L. Jones[a], E. Andrew Payzant[d]

[a]Department of Materials Science and Engineering, University of Tennessee Knoxville, Knoxville, TN, USA
[b]Materials Science and Technology Division, Oak Ridge National Laboratory, Oak Ridge, TN, USA
[c]Research Accelerator Division, Oak Ridge National Laboratory, Oak Ridge, TN, USA
[d]Neutron Scattering Science Division, Oak Ridge National Laboratory, Oak Ridge TN, USA

Received 17 May 2013; received in revised form 21 June 2013; accepted 29 June 2013
Available online 18 July 2013

Abstract

Room temperature and high temperature x-ray powder diffraction and differential thermal analysis/thermo-gravimetric analysis (DTA/TGA) have been used to characterize the phase evolution of bulk mayenite ($Ca_{12}Al_{14}O_{33}$) prepared using the citrate sol–gel method. These studies have shown that single phase mayenite forms at 900 °C in air after approximately three hours. High temperature x-ray powder diffraction data show that when firing in air at temperatures 600 °C and below only amorphous content is observed; above 600 °C $CaCO_3$ is the first phase to crystallize. For samples quenched at 800 °C and evaluated using room temperature x-ray powder diffraction mayenite, $CaAl_2O_4$, and $CaCO_3$ were present. High temperature x-ray diffraction data collected while firing in 4% H_2/96% N_2 reveals that $CaCO_3$ does not form and $Ca_{12}Al_{14}O_{33}$ starts to form around 850 °C. DTA/TGA data collected either in a nitrogen environment or air on samples synthesized using the citrate gel method support the complete decomposition of metastable phases and the formation of mayenite at 900 °C, although the phase evolution is different depending on the environment.

Keywords: B. High temperature X-ray; A. Citrate sol–gel; C. Thermal expansion; B. Scanning electron microscopy

1. Introduction

The mineral mayenite ($Ca_{12}Al_{14}O_{33}$), historically studied as a common phase present in Portland cement, has recently enjoyed renewed research interest due to the discovery of oxygen mobility [1–4], ionic conductivity [5–8], and catalytic properties [9,10]. The physical properties observed in mayenite are related to its crystal structure. The crystal structure is cubic with a unit cell edge of approximately 12 Å and has a Z (formula units) of 2 [5] and is comprised of both nano-pores and polyhedra that form cages (similar to zeolites). Boysen et al. [11] have studied the mayenite structure in detail and call attention to the fact that the formula $Ca_{12}Al_{14}O_{33}$ refers to a unique feature of the anion diffusion process, 64 of the 66 oxygen ions per unit cell are fixed in a Ca–Al–O framework forming 12 "cages", while the other two oxygen ions are distributed within the cages, the formula can be written as

$$[Ca_{12}Al_{14}O_{32}]^{2+}+O^{2-} \quad (1)$$

Boysen et al. [11] describe the cages as approximately 5 Å in diameter and the openings between them are approximately 3.5 Å and have suggested that these openings control the mass transport between the inner cages and the outside. On average each cage has a mean effective charge of +1/3. The free oxygen anions compensate for this positive charge of the framework and are loosely bound to the framework. There is flexibility for the substitution of the free O^{2-} ions with other anions such as fluoride, chloride, hydroxides or hydride, as well as electrons, forming electrides [2,12–17]. Another application, in addition to being an electride, is the generation of negative O^- used in chemical syntheses and materials modifications [18,19].

Mayenite has been prepared in various ways, with solid-state synthesis being the commonly used method. Wet chemistry

*Corresponding author. Tel.: +1 865 974 5340.
E-mail addresses: crawn@utk.edu, rawncj@ornl.gov (C.J. Rawn).

0272-8842/$ - see front matter © 2013 Elsevier Ltd and Techna Group S.r.l. All rights reserved.
http://dx.doi.org/10.1016/j.ceramint.2013.06.112

routes are becoming popular especially sol–gel synthesis. Sol–gel technique involves the conversion of a solution of molecular precursors by a chemical reaction into a sol or a gel, which is transformed into a crystalline material upon drying and subsequently firing [20]. Synthesis steps are performed under ambient conditions, involving no difficult technical challenges in terms of instrumentation or special environment. Furthermore, it ensures adequate and homogenous mixing of the raw materials, and the produced gel can easily be deposited as thin film on a substrate. In this work, citrate sol–gel method, which is simple and cost-effective, has been used to prepare pure phase bulk mayenite at a temperature of 900 °C in about one to three hours; and the phase evolution studied using high temperature x-ray diffraction.

2. Materials and methods

2.1. Synthesis

The starting materials for the solid-state synthesis were powders of $CaCO_3$ (Fisher Chemicals, 99%) and γ-Al_2O_3 (Alfa Aesar, 99.5%). The powders were appropriately weighed out and thoroughly mixed with an agate mortar and pestle, using methanol. After drying the powder was pressed into a pellet using a 13 mm die. The pellet was fired in an alumina crucible at 1200 °C for 16 h, and then reground in the agate mortar and pestle, re-pressed, and fired at 1350 °C for 23.5 h then air quenched. The starting materials for the citrate gel technique included $Ca(NO_3)_2 \cdot 4H_2O$ (Fisher Chemical, 99.5%), $Al(NO_3)_3 \cdot 9H_2O$ (Fisher Chemical, 98.9%), and citric acid ($C_6H_8O_7$) (Alfa Aesar, 99%). The citric acid is a type of weak alpha-hydroxycarboxylic acid that has the ability to form polybasic acid chelates with various cations [21]. This ensures cations to be uniformly distributed in the mixture. Appropriate amounts of nitrates were measured and dissolved in de-ionized water; the solution was heated on a hot plate up to 60 °C before pouring in the citric acid. The citrate–nitrate mixture was heated and vigorously stirred with magnetic stir bar at 90 °C until a gel was formed (about 4–7 h). The resulting gel was placed in a drying oven slightly above 100 °C to dry off the H_2O, and the gel transformed into a cake-like structure, which was subsequently crushed into powder using an agate mortar and pestle. The powder was then divided for the ex-situ and in-situ firing. The samples for the ex-situ experiments were pressed into four pellets. The pellets were each fired at various temperatures (T=1100, 1000, 900 and 800 °C) for 4 h in alumina crucibles. All samples were air quenched and ground by hand in the agate mortar and pestle for subsequent phase identification using x-ray powder diffraction. The powder for the in-situ experiments was pre-calcined at 450 or 600 °C. Chart 1 illustrates the steps of the citrate gel synthesis.

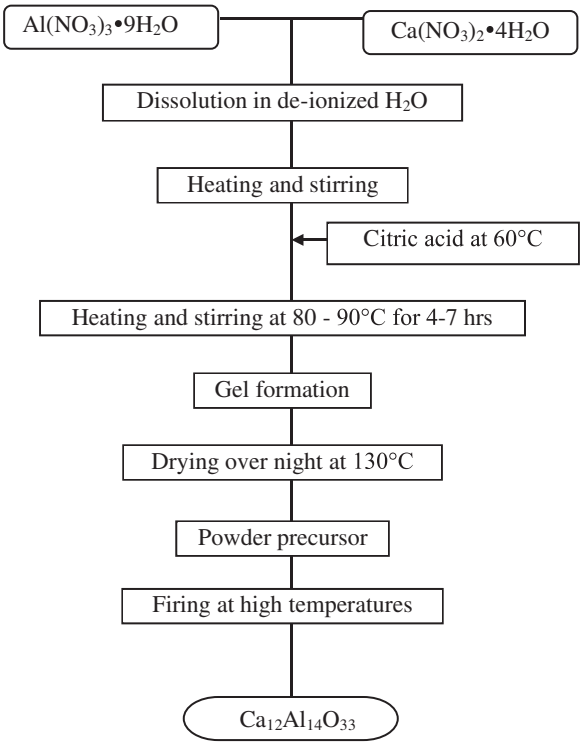

Chart 1. Flow chart of the citrate gel synthesis of mayenite .

2.2. Characterization

X-ray powder diffraction was used to characterize the resulting powders. The data were collected on a PANalytical X′Pert PRO MPD θ–θ diffractometer equipped with an X′celerator Real Time Multiple Strip (RTMS) detector that allows ultrafast data collection. The system was operated at 45 kV and 40 mA using Cu Kα radiation. The data were collected over a range of 10°–75° 2θ with a 0.017° step size and a count time set so that each data collection lasted approximately 12 min. Data for Rietveld refinements were collected using longer count times. An Anton Paar HT16 environmental chamber with a platinum strip heater was used for the in-situ studies. Due to thermal gradients along the strip where both ends of the strip heater are water-cooled, and thermal gradients between the sample and the strip due to interfacial thermal contact resistance between the sample and the strip, as well as contributions dues to the thermal conductivity of the sample, a temperature calibration was performed using Al_2O_3 and MgO standards in order to verify the accurate temperature readings. Additionally, an optical pyrometer was used to determine the temperature of the powder during the study. Data were collected in both air and flowing 4% H_2/96% N_2. Quantitative phase amounts were determined from Rietveld refinements performed using the EXPGUI graphical interface [22] for the General Structure Analysis System (GSAS) [23]. Jade [Jade 6.0, Materials Data Inc.] and HighScore [X′Pert HighScore Plus 3.0, PANalytical, Inc.] software packages were used for phase identification.

Differential Thermal Analysis (DTA) and Thermal Gravimetric Analysis (TGA) were conducted using a TA Instruments SDT Q600 (simultaneous TGA/DSC) at a rate of 5 °C/min with either nitrogen or compressed air as the purging gas. A digital optical microscope (Keyence Digital Microscope, VHX – 1000) was used to look at the dispersion and thickness of citrate gel prepared mayenite powder deposited on a sapphire substrate. The powder

was made into suspension by mixing with ethylene glycol and was deposited on the substrate using a pipette. It was dried over night in the oven at 130 °C and fired at 1100 °C for one hour. The film was x-rayed before and after firing. Scanning Electron Microscopy (SEM) analysis was conducted on the solid-state sample fired at 1350 °C and the citrate gel sample fired at 1100 °C. Micrographs were collected using a LEO 1525 Field Emission Scanning Electron Microscope.

3. Results and discussion

3.1. Physical properties

Observed qualitative physical properties of the pellets after firing included changes in size and color. As expected the pellet size decreased, with the citrate gel generated samples showing a significant reduction in size due, in part, to the loss of evolved gaseous compounds such as NO_2, CO_2, NO, etc. The decrease in weight is confirmed by the thermo-gravimetric analysis results presented in Fig. 1a, with about 34 wt% of the sample remaining after the analysis. All samples synthesized using the citrate gel technique and fired in air were white after firing at temperatures above 800 °C, and the sample fired at 800 °C was gray suggesting that at this temperature the sample did not reach equilibrium. Firing the pellets in a reducing atmosphere resulted in a black color. The citrate gel samples were easier to grind by hand compared to the solid-state samples.

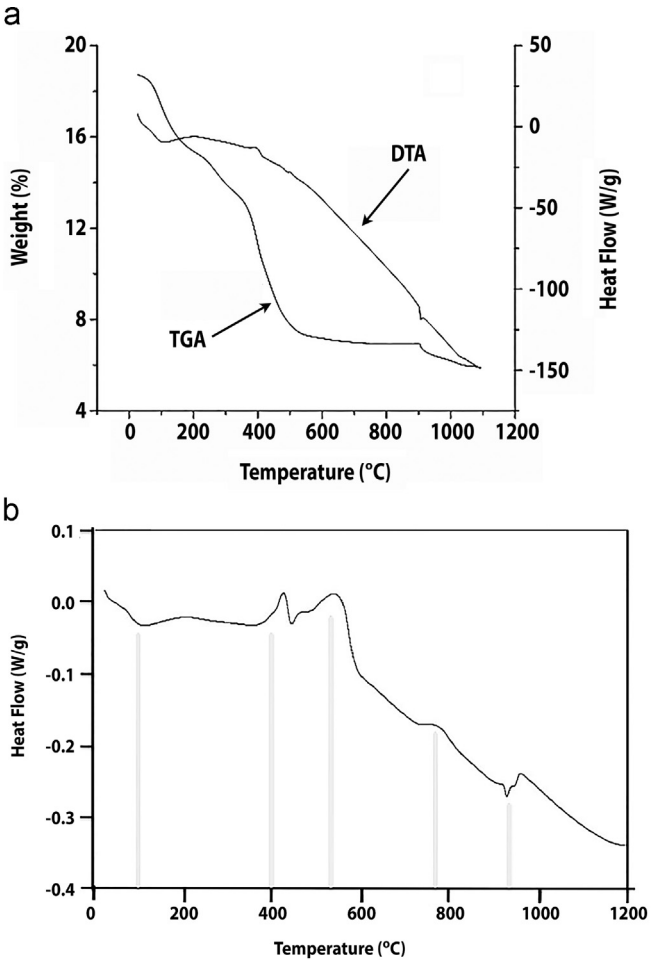

Fig. 1. DTA/TGA curves of mayenite synthesized using the citrate gel method collected in (a) a nitrogen environment and (b) compressed air environment.

3.2. Thermal analysis

The thermo-gravimetric/differential thermal analysis data collected on mayenite synthesized using the citrate gel method, in a nitrogen environment are shown in Fig. 1a. Three areas of major weight changes in the TG graph and the corresponding peaks in the DTA graph are observed. The first peak is at approximately 100 °C resulting from the evaporation of water; the second peak is at approximately 400 °C, possibly resulting from the decomposition of the nitrates and burning off of other organic compounds, and the third peak is at approximately 900 °C suggesting the complete decomposition of all meta-stable phases and formation of mayenite. Fig. 1b is a graph of the DTA data collected, in flowing air, on mayenite synthesized using the citrate gel method. The graph shows more peaks compared to the data collected in nitrogen. The endothermic peak at above 100 °C was attributed to the evaporation of physically absorbed water, followed by decomposition of citric acid below 200 °C. The exothermic peak at around 490 °C was attributed to the oxidation of free carbon resulting from incomplete combustion of the citric acid [24]. At around 400 °C $Al(NO_3)_3$ decomposes into Al_2O_3 and nitrous oxides [25], while $Ca(NO_3)_2$ decomposes into CaO, NO_2, and O_2 around 561 °C [26]. The exothermic peak around 750 °C indicates the transition of amorphous to crystalline phase with the formation of $CaCO_3$, this was also observed in the x-ray results discussed later. The peaks below and above 900 °C suggest decomposition of $CaCO_3$ initially formed from CO_2 from the citric acid and CaO from calcium nitrate, and complete decomposition of all meta-stable phases and formation of mayenite.

3.3. Ex-situ XRD

Ex-situ x-ray powder diffraction data collected on the citrate sol–gel sample fired in air at 800 °C showed $Ca_{12}Al_{14}O_{33}$, $CaAl_2O_4$, and $CaCO_3$, along with a high background suggesting the presence of amorphous content. After re-firing at 800 °C in air for four hours, the x-ray data collected showed a lower background and changes in the fractions of each phase, $Ca_{12}Al_{14}O_{33}$ (79.6 wt%), $CaAl_2O_4$ (14.0 wt%) and $CaCO_3$ (6.4 wt%) confirming that several firings at that temperature are necessary to reach equilibrium. The ex-situ x-ray powder diffraction data, collected on the samples synthesized by the citrate gel method and fired in air at 900, 1000 and 1100 °C and subsequently quenched, all showed single-phase mayenite indicating that the approximate minimum temperature to obtain a single phase is 900 °C. Fig. 2 compares the ex-situ x-ray powder diffraction data for the samples fired in air at 800 and 900 °C, and clearly shows that the sample fired at 900 °C is single phase while the sample fired at 800 °C contains multiple phases.

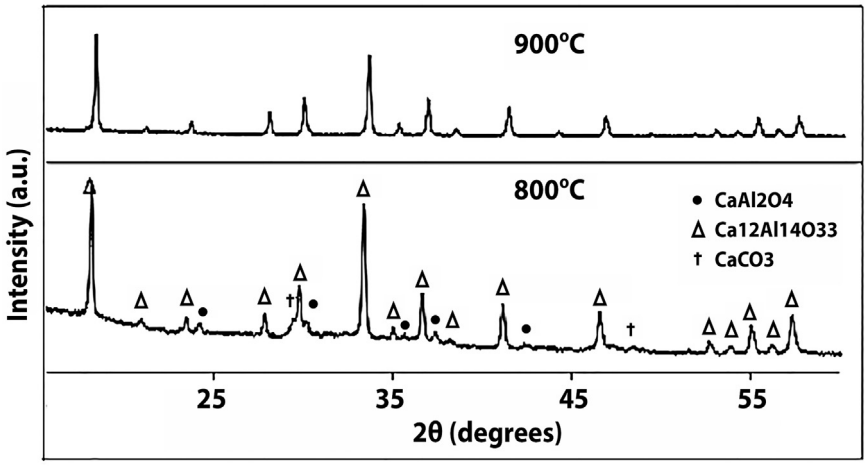

Fig. 2. Ex situ x-ray powder diffraction pattern collected on mayenite synthesized using the citrate gel method and fired in air at 800 and 900 °C.

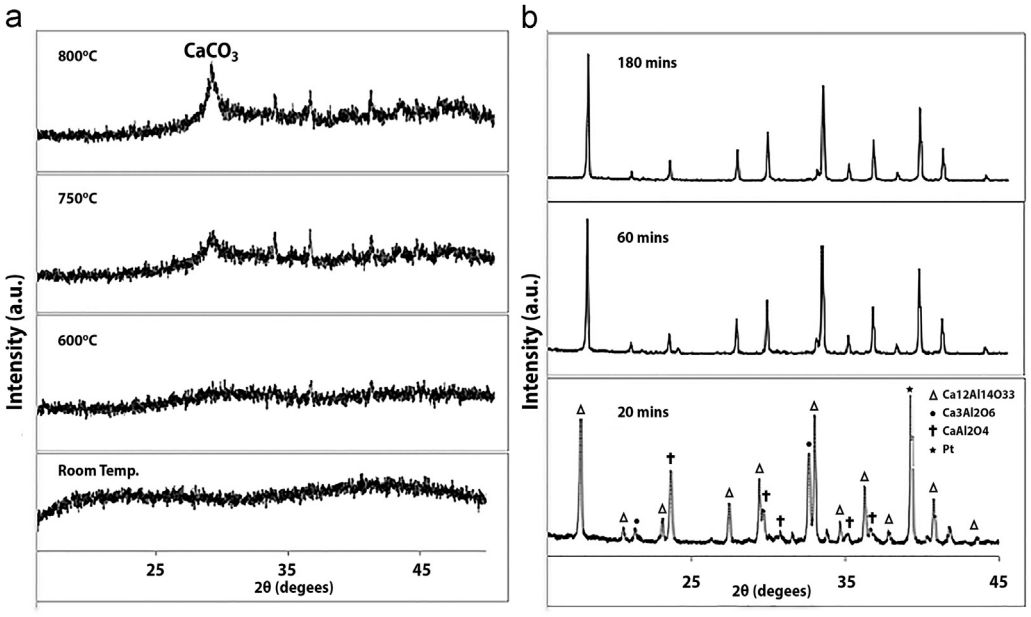

Fig. 3. In-situ x-ray powder diffraction pattern of mayenite synthesized using the citrate gel method, fired in air (a) at room temperature, 600, 750 and 800 °C, and (b) at 850 °C over time.

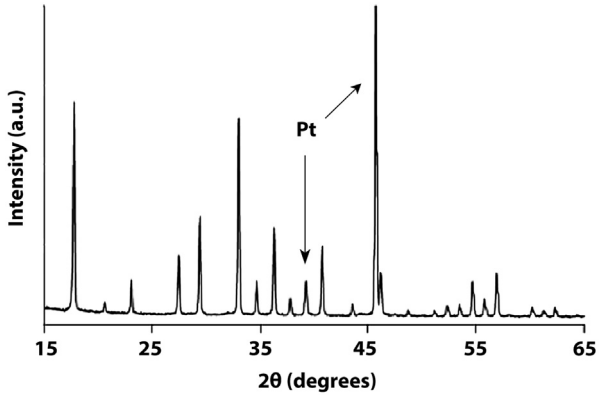

Fig. 4. In-situ x-ray powder diffraction pattern of mayenite synthesized using the citrate gel method, fired in air at 900 °C.

3.4. In-situ XRD

In-situ x-ray diffraction data collected in air at temperatures of 600 °C and below show only amorphous content; however, data collected at higher temperatures indicate the first phase to crystallize is $CaCO_3$ around 750 °C, while the alumina content remains amorphous. Fig. 3a compares the in-situ x-ray powder diffraction data for citrate gel samples at room temperature, 600, 750 and 800 °C. Fig. 3b shows in-situ x-ray data collected at 850 °C over time. At 850 °C, $Ca_{12}Al_{14}O_{33}$, $Ca_3Al_2O_6$ and $CaAl_2O_4$ are present. The $CaAl_2O_4$ phase disappeared over time leaving mayenite (99.1 wt%) as the dominant phase with some amount of $Ca_3Al_2O_6$ (0.9 wt%) present. The in-situ x-ray diffraction data collected at 900 °C after 40 min shows a pure phase

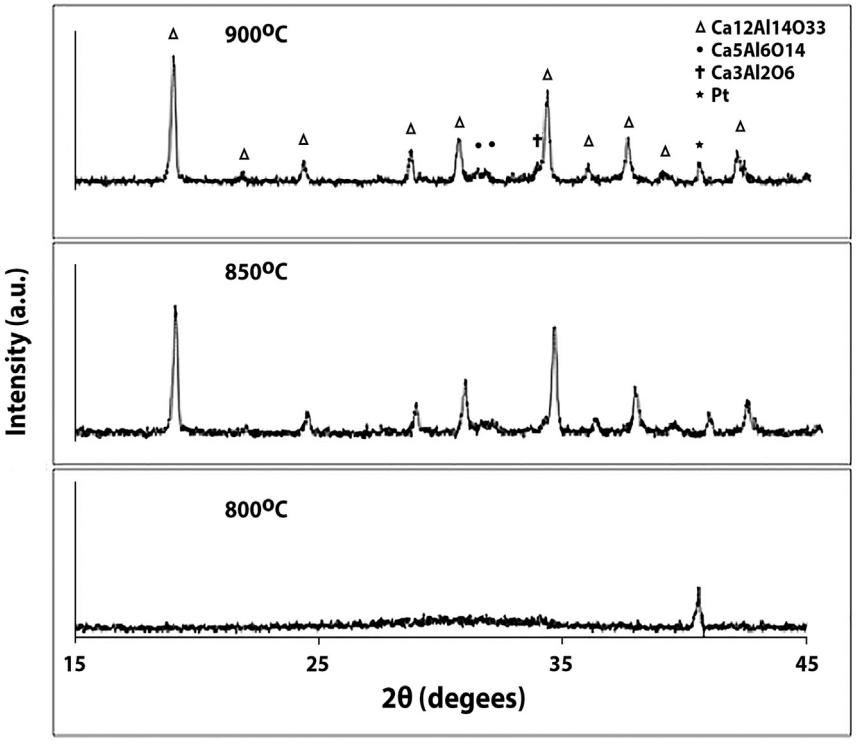

Fig. 5. X-ray powder diffraction pattern of mayenite synthesized using the citrate gel method and fired in 4% H_2/96% N_2 at 800, 850 and 900 °C.

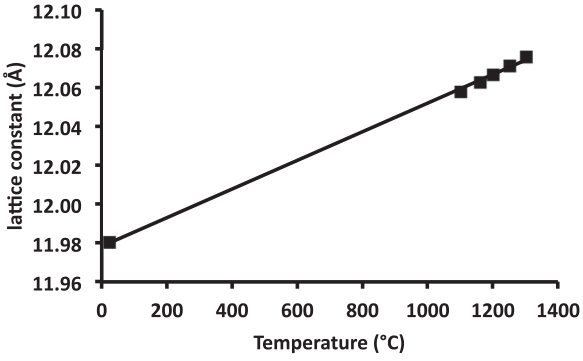

Fig. 6. Refined lattice parameter of mayenite synthesized using the citrate gel method and fired at various temperatures.

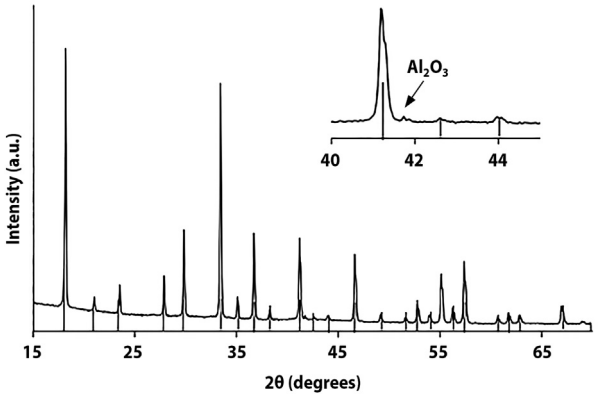

Fig. 7. X-ray powder diffraction pattern of mayenite film deposited on a sapphire substrate.

mayenite as depicted in Fig. 4, confirming that the minimum temperature to achieve phase purity when firing in air is 900 °C. The two Pt peaks shown in the figure are from the platinum strip heater used during the experiment. Fig. 5 compares in-situ x-ray powder diffraction data of citrate gel synthesized samples when fired in 4% H_2/96% N_2 at 800, 850 and 900 °C. The data collected in 4% H_2/96% N_2 does not show the presence of $CaCO_3$, and $Ca_{12}Al_{14}O_{33}$ is the first phase to form around 850 °C. At this temperature a minor amount of $Ca_5Al_6O_{14}$ was observed and the amount increased to 11.7 wt% when the temperature was at 900 °C. The presence of $Ca_3Al_2O_6$ detected in samples fired in both air and 4% H_2/96% N_2 is most likely due to slight errors of the starting ratios (e.g. possibly from excess H_2O in the precursors since the nitrates are highly hygroscopic).

Fig. 6 shows the lattice parameters refined from the x-ray powder diffraction data collected on mayenite synthesized using the citrate sol–gel method and fired in-situ in air. The lattice constant was found to be 11.978 Å at room temperature, close to the literature value [5], and it increased linearly with increasing temperature. The linear thermal expansion coefficient was calculated to be 6.12×10^{-6} K^{-1} and is in good agreement with value reported by Boysen et al. [27].

3.5. Microscopy

X-ray powder diffraction data collected on the mayenite film deposited on the sapphire substrate showed no

structural changes when compared to the data collected on the mayenite powder before deposition. However, the diffraction pattern collected after the deposition showed a minor extra peak, arising from the sapphire substrate, at around $2\theta = 42^{\circ}$. The diffraction pattern is shown in Fig. 7 and the inset shows the peak from the sapphire substrate.

The image of the deposited film under a digital optical microscope is shown in Fig. 8a while Fig. 8b shows a topographical view of the film with one end scrapped in order to determine the thickness of the film. From the image the thickness of the film is seen to be less than 200 μm.

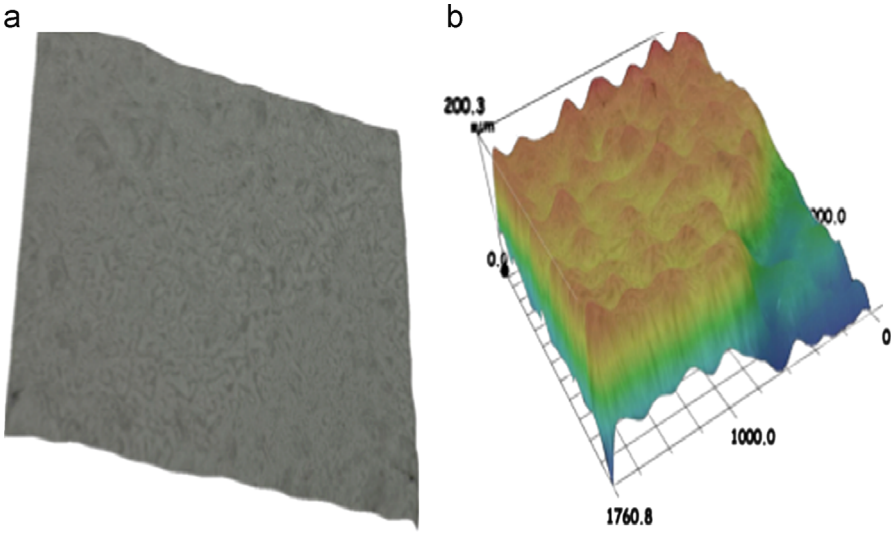

Fig. 8. Digital optical images of deposited mayenite film on sapphire substrate (a) flat view (b) cross-sectional view.

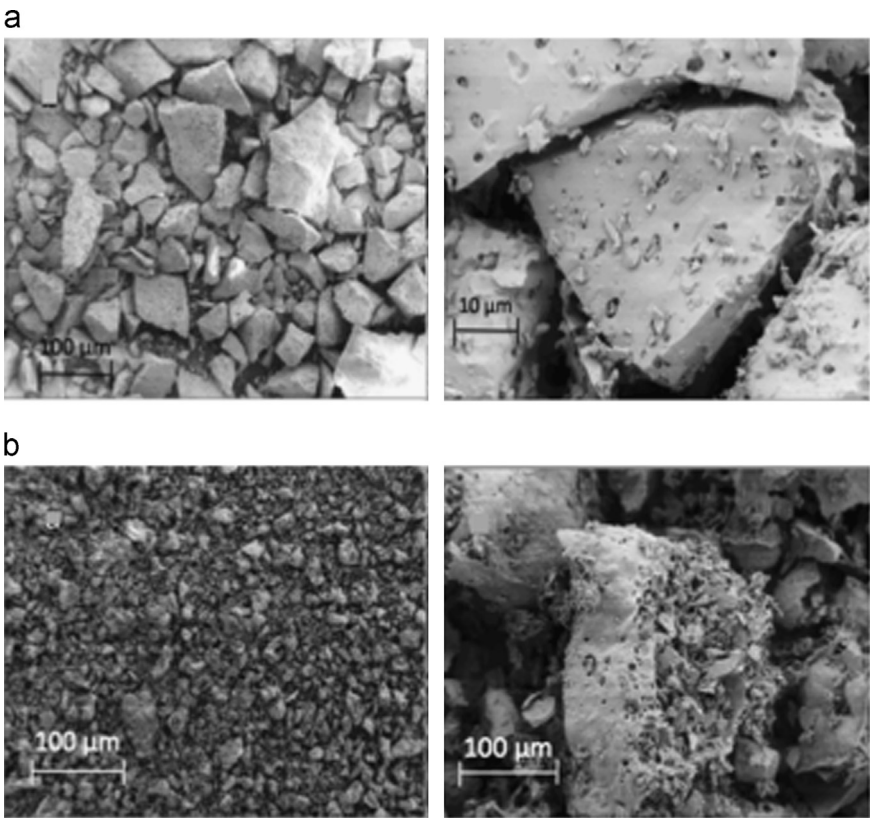

Fig. 9. SEM micrographs of (a) solid-state synthesized mayenite fired at 1350 °C and taken at 100 × (left) and 1000 × (right), and (b) citrate gel synthesized mayenite fired at 1100 °C and collected at 100 × (left) and 1000 × (right).

Fig. 9 shows SEM images collected at different magnifications for the solid-state and citrate sol–gel samples, respectively. The micrographs show randomly shaped particles from samples synthesized using both techniques. The particles produced using the citrate sol–gel technique were smaller compared to particles produced using the solid-state synthesis.

4. Conclusions

High temperature x-ray diffraction data collected on samples synthesized using the citrate gel technique in-situ in air at temperatures of 600 °C and below showed only amorphous content; however, data collected at higher temperatures indicated the first phase to crystallize is $CaCO_3$ and when fired in air at 800 °C showed multiple phases including calcite. When fired at 900 °C or above x-ray powder diffraction data showed single-phase mayenite. In contrast high temperature x-ray diffraction data collected in 4% H_2/96% N_2 does not show the presence of $CaCO_3$, and $Ca_{12}Al_{14}O_{33}$ starts to form around 850 °C. DTA/TGA data support unique phase evolution paths for the two different environments. Particles produced by the citrate gel method show more and smaller pores compared to particles synthesized using the solid-state technique. Citrate sol–gel synthesis proves to be a good technique for producing mayenite requiring less time and lower temperatures, without subsequent firings in order to reach equilibrium.

Acknowledgments

SNU was partly supported by Pipeline Engineering Diversity Program under DOE grant DE-FG02-05ER25717, and partly sponsored by the Center for Materials Processing (CMP) at the University of Tennessee. X-ray powder diffraction data were collected at the High Temperature Materials Laboratory at Oak Ridge National Laboratory, which is sponsored by the US Department of Energy, Office of Energy Efficiency and Renewable Energy, Vehicle Technologies Program. A portion of this research was conducted at the Center for Nanophase Materials Sciences, sponsored at Oak Ridge National Laboratory by the Scientific User Facilities Division, Office of Basic Energy Sciences, US Department of Energy. The authors would like to thank Austin Albert for his help with the BET data collection and analysis.

References

[1] S. Fujita, M. Ohkawa, K. Suzuki, H. Nakano, T. Mori, H. Masuda, Controlling the quantity of radical oxygen occluded in a new aluminum silicate with nanopores, Chemistry of Materials 15 (26) (2003) 4879–4881.
[2] Z. Li, J. Yang, J.G. Hou, Q. Zhu, Is mayenite without clathrated oxygen an inorganic electride?, Angewandte Chemie International Edition 43 (47) (2004) 6479–6482.
[3] P.V. Sushko, A.L. Shluger, K. Hayashi, M. Hirano, H. Hosono, Mechanisms of oxygen ion diffusion in a nanoporous complex oxide $12CaO{\cdot}7Al_2O_3$, Physical Review B 73 (1) (2006) 014101.
[4] K. Hayashi, N. Ueda, S. Matsuishi, M. Hirano, T. Kamiya, H. Hosono, Solid state syntheses of $12SrO{\cdot}7Al_2O_3$ and formation of high density oxygen radical anions, O^- and O^{2-}, Chemistry of Materials 20 (19) (2008) 5987–5996.
[5] S. Matsuishi, Y. Toda, M. Miyakawa, K. Hayashi, T. Kamiya, M. Hirano, I. Tanaka, H. Hosono, High-density electron anions in a nanoporous single crystal: $[Ca_{24}Al_{28}O_{64}]^{4+}(4e^-)$, Science 301 (5633) (2003) 626–629.
[6] Y. Toda, S. Matsuishi, K. Hayashi, K. Ueda, T. Kamiya, M. Hirano, H. Hosono, Field emission of electron anions clathrated in subnanometer-sized cages in $[Ca_{24}Al_{28}O_{64}]^{4+}(4e^-)$, Advanced Materials 16 (8) (2004) 685–689.
[7] T. Kamiya, S. Aiba, M. Miyakawa, K. Nomura, S. Matsuishi, K. Hayashi, K. Ueda, M. Hirano, H. Hosono, Field-induced current modulation in nanoporous semiconductor, electron-doped $12CaO{\cdot}7Al_2O_3$, Chemistry of Materials 17 (25) (2005) 6311–6316.
[8] O. Trofymluk, Y. Toda, H. Hosono, A. Navrotsky, Energetics of formation and oxidation of microporous calcium aluminates: a new class of electrides and ionic conductors, Chemistry of Materials 17 (22) (2005) 5574–5579.
[9] S. Fujita, H. Nakano, K. Suzuki, T. Mori, H. Masuda, Oxidative destruction of hydrocarbons on $Ca_{12}Al_{14-x}Si_xO_{33+0.5x}$ ($0 \le x \le 4$) with radical oxygen occluded in nanopores, Catalysis Letters 106 (3–4) (2006) 139–143.
[10] C. Li, K. Suzuki, Kinetic analyses of biomass tar pyrolysis using the distributed activation energy model by TG/DTA technique, Journal of Thermal Analysis and Calorimetry 98 (1) (2009) 261–266.
[11] H. Boysen, I. Kaiser-Bischoff, M. Lerch, Anion diffusion processes in O-and N-mayenite investigated by neutron powder diffraction, Diffusion Fundamentals 8 (2) (2008) 1–2.8.
[12] P.V. Sushko, A.L. Shluger, K. Hayashi, M. Hirano, H. Hosono, Electron localization and a confined electron gas in nanoporous inorganic electrides, Physical Review Letters 91 (2003) 126401-1–126401-4.
[13] J.E. Medvedeva, A.J. Freeman, Hopping versus bulk conductivity in transparent oxides: $12CaO{\cdot}7Al_2O_3$, Applied Physics Letters 85 (6) (2004) 955–957.
[14] J.L. Dye, From 1D Heisenberg chains to 2D pseudo-metals, Inorganic Chemistry 36 (18) (1997) 3816–3826.
[15] K. Hayashi, S. Matsuishi, T. Kamiya, M. Hirano, H. Hosono, Light-induced conversion of an insulating refractory oxide into a persistent electronic conductor, Nature 419 (6906) (2002) 462–465.
[16] K. Hayashi, M. Hirano, S. Matsuishi, H. Hosono, Microporous crystal $12CaO{\cdot}7Al_2O_3$ encaging abundant O^- radicals, Journal of the American Chemical Society 124 (5) (2002) 738–739.
[17] K. Hayashi, S. Matsuishi, N. Ueda, M. Hirano, H. Hosono, Maximum incorporation of oxygen radicals, O^- and O^{2-}, into $12CaO{\cdot}7Al_2O_3$ with a nanoporous structure, Chemistry of Materials 15 (9) (2003) 1851–1854.
[18] Q.X. Li, K. Hayashi, M. Nishioka, H. Kashiwagi, M. Hirano, Y. Torimoto, H. Hosono, M. Sadakata, Absolute emission current density of O_2 from $12CaO{\cdot}7Al_2O_3$ crystal, Applied Physics Letters 80 (22) (2002) 4259–4261.
[19] A.S. Tolkacheva, S.N. Shkerin, S.V. Plaksin, E.G. Vovkotrub, K.M. Bulanin, V.A. Kochedykov, D.P. Ordinartsev, O.I. Gyrdasova, N.G. Molchanova, Synthesis of dense ceramics of single-phase mayenite $(Ca_{12}Al_{14}O_{32})O$, Russian Journal of Applied Chemistry 84 (6) (2011) 907–911.
[20] A.K. Cheetham, C.F. Mellot, In situ studies of the sol–gel synthesis of materials, Chemistry of Materials 9 (11) (1997) 2269–2279.
[21] X. Yuan, Y.B. Xu, Y. He, Synthesis of $Ca_3Al_2O_6$ via citric acid precursor, Materials Science and Engineering: A 447 (1–2) (2007) 142–145.
[22] B. Toby, EXPGUI, a graphical user interface for GSAS, Journal of Applied Crystallography 34 (2) (2001) 210–213.
[23] A. Larson, R. Von Dreele, Los Alamos National Laboratory Report LAUR 86-748 (unpublished).
[24] J. Li, Y. Pan, F. Qiu, Y. Wu, J. Guo, Nanostructured Nd:YAG powders via gel combustion: the influence of citrate-to-nitrate ratio, Ceramics International 34 (1) (2008) 141–149.
[25] S. Yuvaraj, L. Fan-Yuan, C. Tsong-Huei, Y. Chuin-Tih, Thermal decomposition of metal nitrates in air and hydrogen environments, Journal of Physical Chemistry B 107 (4) (2003) 1044–1047.
[26] C. Ettarh, A.K. Galwey, Thermal analysis of anhydrous mixtures of calcium nitrate and selected metal oxides, Thermochimica Acta 261 (0) (1995) 125–139.
[27] H. Boysen, M. Lerch, A. Stys, A. Senyshyn, Structure and oxygen mobility in mayenite ($Ca_{12}Al_{14}O_{33}$): a high-temperature neutron powder diffraction study, Acta Crystallographica Section B 63 (5) (2007) 675–682.